

High-Temperature Effective Potential of Noncommutative Scalar Field Theory: Reduction of Degrees of Freedom by Noncommutativity

Wung-Hong Huang
Department of Physics
National Cheng Kung University
Tainan,70101,Taiwan

The renormalization of effective potentials for the noncommutative scalar field theory at high temperature are investigated to the two-loop approximation. The Feynman diagrams in evaluating the effective potential may be classified into two types: the planar diagrams and nonplanar diagrams. The nonplanar diagrams, which depend on the parameter of noncommutativity, do not appear in the one-loop potential. Despite their appearance in the two-loop level, they do not have an inclination to restore the symmetry breaking in the tree level, in contrast to the planar diagrams. This phenomenon is explained as a consequence of the drastic reduction of the degrees of freedom in the nonplanar diagrams when the thermal wavelength is smaller than the noncommutativity scale. Our results show that the nonplanar two-loop contribution to the effective potential can be neglected in comparison with that from the planar diagrams.

E-mail: whhwung@mail.ncku.edu.tw

Keywords: Superstrings and Heterotic String, Non-commutative Geometry.

PACS:11.10.Lm; 11.10.Kk; 11.10.Wx; 12.38.Bx

1 Introduction

Field theory on noncommutative space (or spacetime) has received a great deal of attention recently. Initially, Connes, Douglas and Schwarz [1] showed that the supersymmetric gauge theory on noncommutative torus is naturally related to the compactification of Matrix theory. From string theory, it was also found that the end points of the open strings trapped on a D-brane with a nonzero NSNS two form B-field background turns out to be noncommuting [2-4]. As it has proved to arise naturally in the string/M theory the noncommutative field theory has attracted many researchers [5-18].

The quantum field theories on the noncommutative space (or spacetime) have been pursued via perturbative analysis over diverse model. The noncommutative scalar field theory have been considered in [5-8]. It has been shown that this theory is renormalizable up to two loops. The pure noncommutative gauge theory has also been shown to be renormalizable up to one loop [9,10]. Historically it was a hoped that introducing a minimum scale to deform the geometry in the small spacetime would be possible to cure the quantum-field divergences, especially in the gravity theory [11,12]. Although the noncommutative field theory turns out to exhibit the same divergence as the commutative one [5], it is of interests in its own right. The special properties of the nonlocality (they contain infinite order derivatives) and the existence of a new parameter (the noncommutativity parameter, θ) in the noncommutative field theories make them challenging and lead to some fascinating behaviors.

A distinct characteristic of the noncommutative field theories, found by Minwalla, Raamsdonk and Seiberg [6], is the mixing of ultraviolet (UV) and infrared (IR) divergences reminiscent of the UV/IR connection of the string theory. The nontrivial mixing between UV and IR is very special and may be explained as the nonlocality shown in the noncommutative spacetime [6].

In recent papers [13,14], it has also been found that the noncommutativity in the extra spaces may be used to stabilize the radius of extra space by the Casimir effect. It seems that the dimensional parameter of space noncommutativity can provide a minimum scale to protect the collapse of the extra space in some systems.

Another interesting characteristic of the appearance of a minimum scale is also found in the finite-temperature noncommutative field theories [15-17]. Fischler *et. al.* [15] showed that, at high temperature for which the thermal wavelength is small than the noncommutativity scale, there is no way to distinguish and count the contributions of modes to the free energy. Thus, there is a drastic reduction of the degrees of freedom in the non-planar contribution to the thermodynamical potential at high temperature.

In this paper we will investigate the renormalized two-loop effective potential for noncommutative scalar field theory in the high-temperature limit. We will see that the property of the reduction of the degrees of freedom found in [15] can also be seen in the effective potential. Note that the free energy evaluated in [15] is given to the second order of coupling constant λ , while the effective potential evaluated in this paper is given to the second order of \hbar and to all order in the coupling λ . As the space-time noncommutativity ($\theta_{0i} \neq 0$) will lead to infinite number of time derivative, it will render the field theory nonlocal in time and the causality may be violated at the quantum level [18]. Therefore we shall in this paper consider only space noncommutative theory.

In section 2, we briefly review the relation between the field theory on noncommutative spacetime and the noncommutative field theory. The path-integration formulation of Jackiw [19,20], which is used to evaluate the effective potential, is then extended to the noncommutative theory and the Feynman diagrams are derived. In this section we see that the spacetime noncommutativity does not affect the one-loop potential. Thus the radiatively symmetry breaking is blind to the noncommutativity at this level [5,8]. It is seen that this property is independent of the spacetime dimension and irrelevant to temperature.

The Feynman rule derived in section 2 is then used to analyze the two-loop diagram of the $\lambda\phi^4$ theory at high temperature. The Feynman diagrams therein may be classified as two types: the planar diagrams and nonplanar diagrams. The nonplanar diagrams are the parts which will depend on the parameter of space noncommutativity. They appear in the two-loop level but do not have an inclination to restore the symmetry breaking in the tree level. This property is in contrast to the conventional believing that high temperature could restore the symmetry breaking. To explain this phenomenon we compare the result with the effective potential in the zero-space dimension and explain this property as a consequence of drastic reduction of the degrees of freedom in the nonplanar diagrams at high temperature in which the thermal wavelength is smaller than the noncommutativity scale [15]. Our results, however, show that the nonplanar two-loop contribution to the effective potential can be neglected in comparing to that from the planar diagrams.

To confirm the above argument of the drastic reduction of the degrees of freedom in the nonplanar diagram at high temperature, we present in section 4 an analysis of the two-loop effective potential of the $\lambda\phi^3$ theory at high temperature. In the last section we give a short conclusion.

2 Formulation

2.1 Quantum Field on Noncommutative Spacetime

We consider the noncommutative geometry \mathcal{R}^n defined in n dimensions with the commutations

$$[\hat{x}^\mu, \hat{x}^\nu] = i\theta^{\mu\nu}, \quad (2.1)$$

where $\theta^{\mu\nu}$ are real C-numbers. Given this algebra we can follow the method of Weyl [21] to describe the functions living on the noncommutative spacetime. The method is to define the function

$$\hat{f}(\hat{x}) = \frac{1}{(2\pi)^{n/2}} \int d^n k e^{ik_\mu \hat{x}^\mu} \tilde{f}(k), \quad (2.2)$$

where $\tilde{f}(k)$ is the Fourier transform of $f(x)$:

$$\tilde{f}(k) = \frac{1}{(2\pi)^{n/2}} \int d^n x e^{-ik_\mu x^\mu} f(x), \quad (2.3)$$

in which x is the commuting variable corresponding the noncommuting variable \hat{x} . This definition uniquely associates a function $\hat{f}(\hat{x})$ living on the noncommutative spacetime

with a function $f(x)$ living on the commutative spacetime. From the above definition the product of two functions $\hat{f}(\hat{x})$ and $\hat{g}(\hat{x})$ then becomes

$$\begin{aligned}\hat{f}(\hat{x}) \cdot \hat{g}(\hat{x}) &= \frac{1}{(2\pi)^n} \int d^n k d^n p e^{ik_\mu \hat{x}^\mu} e^{ip_\nu \hat{x}^\nu} \tilde{f}(k) \tilde{g}(p) \\ &= \frac{1}{(2\pi)^n} \int d^n k d^n p e^{i(k_\mu + p_\mu) \hat{x}^\mu - \frac{i}{2} k_\mu \theta^{\mu\nu} p_\nu} \tilde{f}(k) \tilde{g}(p).\end{aligned}\quad (2.4)$$

To obtain the above relation we have used the Baker-Campbell-Hausdorff formula

$$e^A e^B = \exp\left(A + B + \frac{1}{2}[A, B] + \frac{1}{12}[A, [A, B]] + \frac{1}{12}[B, [B, A]] + \dots\right),$$

and the fact that the commutators $\theta^{\mu\nu}$ are constants, thus the higher commutators vanish. From Eq.(2.4), we see that once we define the Moyal product $(*)$ [22]

$$\begin{aligned}f(x) * g(x) &= \frac{1}{(2\pi)^n} \int d^n k d^n p e^{i(k_\mu + p_\mu)x^\mu} e^{-\frac{i}{2} k_\mu \theta^{\mu\nu} p_\nu} \tilde{f}(k) \tilde{g}(p) \\ &= e^{\frac{i}{2} \theta^{\mu\nu} \frac{\partial}{\partial y^\mu} \frac{\partial}{\partial z^\nu}} f(y) g(z) \Big|_{y, z \rightarrow x},\end{aligned}\quad (2.5)$$

we can establish a homomorphism, $\hat{f}(\hat{x}) \cdot \hat{g}(\hat{x}) = f(x) * g(x)$. This homomorphism allows us to view the algebra of functions on noncommutative spacetime \mathcal{R}^n as the algebra of the ordinary functions on commutative \mathcal{R}^n with the Moyal $*$ -product instead with the usual pointwise product.

Therefore, in investigating the field theory on noncommutative spacetime we can always work on a usual commutative spacetime in which the multiplication operator is replaced by the so called Moyal $*$ product; in other words, we are going to study the problem of noncommutative field theory.

Note that the Moyal $*$ product satisfies the law of associativity:

$$(f(x) * g(x)) * h(x) = f(x) * (g(x) * h(x)). \quad (2.6a)$$

Under the integral it also has a property:

$$\int d^n x (f(x) * g(x)) = \int d^n x (f(x) \cdot g(x)), \quad (2.6b)$$

as the noncommutativity θ is an antisymmetric matrix.

2.2 Path-Integral Formulation of Effective Potential

In this section we will consider the $\lambda\phi^4$ theory on a noncommutative spacetime. Using the above prescription we can write the Lagrangian as

$$S[\phi] = \int d^n x \mathcal{L}(\phi) = \int d^n x \left[\frac{1}{2} \partial_\mu \phi \partial^\mu \phi - \frac{1}{2} m^2 \phi^2 - \frac{\lambda}{4!} \phi * \phi * \phi * \phi \right]. \quad (2.7)$$

We will evaluate the renormalized effective potential of the above model along the path-integration formulation of Jackiw [19,20].

First, we assume that there exists a stationary point at which ϕ is a constant field ϕ_0 . Thus

$$\left. \frac{\delta S}{\delta \phi} \right|_{\phi_0} = 0.$$

Next, we expand the Lagrangian about the stationary point the action becomes

$$S[\phi] = S[\phi_0] + \frac{1}{2} \int d^n x d^n y \tilde{\phi}(x) \star \tilde{\phi}(y) \left. \frac{\delta^2 S}{\delta \phi(x) \delta \phi(y)} \right|_{\phi_0} + \int d^n x \tilde{\mathcal{L}}_{\mathcal{I}}(\tilde{\phi}, \phi_0), \quad (2.8)$$

in which $\tilde{\phi} \equiv \phi - \phi_0$ and $\tilde{\mathcal{L}}_{\mathcal{I}}(\tilde{\phi}, \phi_0)$ can be found from the Lagrangian Eq.(2.7). Then we use the propagator defined by

$$iD^{-1}(\phi_0; p) = \int d^n p e^{ipx} iD^{-1}(\phi_0; x, 0), \quad (2.9a)$$

$$iD^{-1}(\phi_0; x, y) = \left. \frac{\delta^2 S}{\delta \phi(x) \delta \phi(y)} \right|_{\phi_0}, \quad (2.9b)$$

the effective potential $V(\phi_0)$ is found to be [19]

$$V(\phi_0) = V_0(\phi_0) - \frac{1}{2} i \hbar \int \frac{d^n p}{(2\pi)^n} \ln \det [iD^{-1}(\phi_0; p)] + i \hbar \langle \exp \left(\frac{i}{\hbar} \int d^n x \tilde{\mathcal{L}}_{\mathcal{I}}(\tilde{\phi}, \phi_0) \right) \rangle. \quad (2.10)$$

For the theory at finite temperature $T = 1/\beta$ we shall take the following substitutions [20]:

$$p_0 \rightarrow \frac{2\pi p_0}{\beta}, \quad (2.11)$$

$$\int d^n p \rightarrow \frac{2\pi}{\beta} \sum_{p_0} \int d^{n-1} \mathbf{p} \quad (2.12),$$

in which p_0 is an integral.

The first term in Eq.(2.10) is the classical potential which can be read from Eq.(2.7). The second term is the one-loop contribution which comes from the second term in Eq.(2.8). The elementary property (2.6b) implies that the Moyal \star -product in the second term of Eq.(2.8) can be dropped. Thus we see an interesting property that the noncommutativity of spacetime dose not affect the potential in the one-loop level. This property has been found by Campbell and Kaminsky [5] in the investigation of the tadpole diagram in the linear sigma model. It is easy to see that this property is independent of the spacetime dimension and irrelevant to the temperature.

The third term in Eq.(2.10) is the higher-loop contribution of the effective potential. To obtain it one shall evaluate the expectation value of the third term in Eq.(2.8) by the

Feynman rule, with $D(\phi_0; p)$, defined in Eq.(2.9), as the propagator and keep only the connected single-particle irreducible graphs [19,20].

The Feynman rules including the propagator and vertices are shown in figure 1.

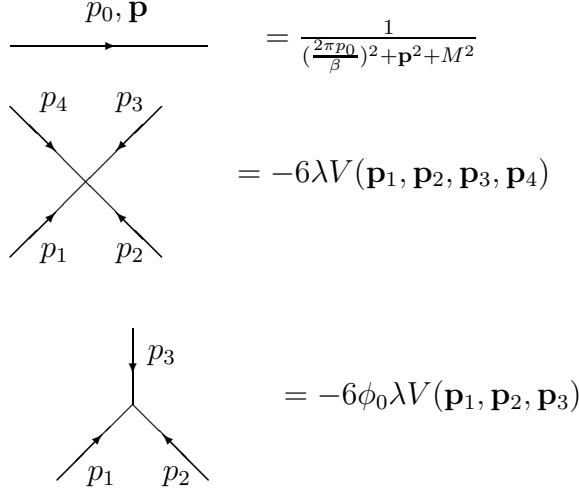


Figure 1. Feynman rules : propagator and vertices

In figure 1 we define

$$M^2 = m^2 + \frac{1}{2}\lambda\phi_0^2, \quad (2.13)$$

and

$$V(\mathbf{p}_a, \mathbf{p}_b, \dots) = \exp \left[\frac{-i}{2} \sum_{a < b} (\mathbf{p}_a)_i \theta^{ij} (\mathbf{p}_b)_j \right]. \quad (2.14)$$

Note that we consider only space noncommutative theories (i.e. $\theta_{0i} = 0$) for the unitarity requirement [18].

In the following sections we will use the above Feynman rules to evaluate the two-loop diagram for the system at high temperature. We will use the zeta-function regularization method [23] to perform the summations over the integral values of p_0 and k_0 .

3 Two-Loop Corrections: $\lambda\phi^4$ Theory

From the Feynman rule we see that the diagrams in the two-loop level can be divided into two types: planar diagrams and nonplanar diagrams. The contributions of the effective potentials from the planar diagrams come from the two diagrams [19,20,8] shown in figure 2.



Figure 2. Planar two-loop contributions to the effective potential

For the theory in 1+3 dimensions the effective potentials evaluated from figure 2 are

$$I_1^P = \frac{2}{3} \frac{\hbar^2 \lambda}{24 \beta^2} \sum_{k_0} \int \frac{d^3 \mathbf{k}}{(2\pi)^3} \frac{1}{\left(\frac{2\pi k_0}{\beta}\right)^2 + \mathbf{k}^2 + M^2} \sum_{p_0} \int \frac{d^3 \mathbf{p}}{(2\pi)^3} \frac{1}{\left(\frac{2\pi p_0}{\beta}\right)^2 + \mathbf{p}^2 + M^2}, \quad (3.1)$$

$$I_2^P = -\frac{1}{2} \frac{\hbar^2 \lambda^2 \phi_0^2}{36 \beta^2} \sum_{k_0} \sum_{p_0} \int \frac{d^3 \mathbf{k}}{(2\pi)^3} \int \frac{d^3 \mathbf{p}}{(2\pi)^3} \frac{1}{\left(\frac{2\pi k_0}{\beta}\right)^2 + \mathbf{k}^2 + M^2} \times \frac{1}{\left(\frac{2\pi p_0}{\beta}\right)^2 + \mathbf{p}^2 + M^2} \frac{1}{\left(\frac{2\pi k_0}{\beta} + \frac{2\pi p_0}{\beta}\right)^2 + (\mathbf{p} + \mathbf{k})^2 + M^2}. \quad (3.2)$$

The contributions from the nonplanar diagrams are like those in the planar diagrams, but with an extra factor $e^{i\mathbf{k}_i \theta^{ij} \mathbf{p}_j}$. They read

$$I_1^N = \frac{1}{3} \frac{\hbar^2 \lambda}{24 \beta^2} \sum_{k_0} \sum_{p_0} \int \frac{d^3 \mathbf{k}}{(2\pi)^3} \int \frac{d^3 \mathbf{p}}{(2\pi)^3} \frac{e^{i\mathbf{k}_i \theta^{ij} \mathbf{p}_j}}{\left[\left(\frac{2\pi k_0}{\beta}\right)^2 + \mathbf{k}^2 + M^2\right] \left[\left(\frac{2\pi p_0}{\beta}\right)^2 + \mathbf{p}^2 + M^2\right]}, \quad (3.3)$$

$$I_2^N = -\frac{1}{2} \frac{\hbar^2 \lambda^2 \phi_0^2}{36 \beta^2} \sum_{k_0} \sum_{p_0} \int \frac{d^3 \mathbf{k}}{(2\pi)^3} \int \frac{d^3 \mathbf{p}}{(2\pi)^3} \frac{1}{\left(\frac{2\pi k_0}{\beta}\right)^2 + \mathbf{k}^2 + M^2} \times \frac{1}{\left(\frac{2\pi p_0}{\beta}\right)^2 + \mathbf{p}^2 + M^2} \frac{e^{i\mathbf{k}_i \theta^{ij} \mathbf{p}_j}}{\left(\frac{2\pi k_0}{\beta} + \frac{2\pi p_0}{\beta}\right)^2 + (\mathbf{p} + \mathbf{k})^2 + M^2}. \quad (3.4)$$

Note that the factors $\frac{2}{3}$ ($\frac{1}{3}$) appearing in Eqs. (3.1) ((3.3)) means that the associated planar (nonplanar) diagram will be with 2/3 (1/3) weight of the commutative graph. And the factor $\frac{1}{2}$ appearing in Eqs. (3.2) and (3.4) means that the associated planar and nonplanar diagrams will both have weight of 1/2 of the commutative graph. The counting rule has been detailed by Campbell and Kaminsky [5] in the investigation of the linear sigma model. Let us describe it again for completeness.

The diagram (3.1) has a single vertex, and so has a phase factor $V(p, k, -k, -p)$. Of the six possible orderings (modulo cyclic permutation) of the set $\{p, k, -k, -p\}$, four have a trivial phase factor, and two have a phase of either $e^{i\mathbf{k}_i \theta^{ij} \mathbf{p}_j}$ or $e^{-i\mathbf{k}_i \theta^{ij} \mathbf{p}_j}$ (which are the same under the integral over the loop momenta k). Thus the planar diagrams will have 4/6=2/3 weight and the nonplanar diagrams will have 2/6=1/3 weight with respect to the commutative graph. .

The diagram (3.2) has two vertices, and we pick up the phase factor $V(p, k, -p - k)V(-k, -p, p + k)$. Each vertex has two orderings (modulo cyclic permutation), for four combinations in total. Explicitly evaluation leads to two having a trivial phase factor, and another two having a phase $e^{i\mathbf{k}_i \theta^{ij} \mathbf{p}_j}$. Thus the planar diagrams will with 2/4=1/2 weight and the nonplanar diagrams will with 2/4=1/2 weight with respect to the commutative graph.

3.1 Nonplanar Diagrams

We first analyze the nonplanar diagrams. Using the Schwinger parameters, α_1 and α_2 , that in Eq. (3.3) can be expressed as

$$\begin{aligned}
& \frac{1}{\beta^2} \sum_{k_0} \sum_{p_0} \int d^3 \mathbf{k} d^3 \mathbf{p} \frac{e^{i \mathbf{k}_i \theta^{ij} \mathbf{p}_j}}{\left[\left(\frac{2\pi k_0}{\beta} \right)^2 + \mathbf{k}^2 + M^2 \right] \left[\left(\frac{2\pi p_0}{\beta} \right)^2 + \mathbf{p}^2 + M^2 \right]} \\
&= \frac{1}{\beta^2} \int_0^\infty d\alpha_1 \int_0^\infty d\alpha_2 \sum_{p_0} \sum_{l_0} \int d^3 \mathbf{p} d^3 \mathbf{l} e^{-\frac{1}{4\alpha_1} \tilde{\mathbf{p}}_i \tilde{\mathbf{p}}^i} e^{-\alpha_1 \left[\left(\frac{2\pi p_0}{\beta} \right)^2 + \mathbf{p}^2 + M^2 \right]} e^{-\alpha_2 \left[\left(\frac{2\pi l_0}{\beta} \right)^2 + \mathbf{l}^2 + M^2 \right]} \\
&= \frac{1}{\beta^2} \int_0^\infty d\alpha_1 \int_0^\infty d\alpha_2 \left(\frac{\pi}{\alpha_1} \right)^{\frac{3}{2}} e^{-(\alpha_1 + \alpha_2) M^2} \int d^3 \mathbf{p} e^{-\frac{1}{4\alpha_1} \tilde{\mathbf{p}}_i \tilde{\mathbf{p}}^i} e^{-\alpha_2 \mathbf{p}^2} \sum_{p_0} e^{-\alpha_1 \left(\frac{2\pi p_0}{\beta} \right)^2} \sum_{l_0} e^{-\alpha_2 \left(\frac{2\pi l_0}{\beta} \right)^2}, \tag{3.5}
\end{aligned}$$

in which $\tilde{\mathbf{p}}^i = \theta^{ij} \mathbf{p}_j$ and $\mathbf{l}_j = \mathbf{k}_j - \frac{i}{2\alpha_1} \tilde{\mathbf{p}}_j$.

In the same way, using the Feynman parameter w , the Schwinger parameters, α_1 and α_2 , that in Eq. (3.4) can be expressed as

$$\begin{aligned}
& \frac{1}{\beta^2} \sum_{k_0} \sum_{p_0} \int d^3 \mathbf{k} d^3 \mathbf{p} \frac{1}{\left(\frac{2\pi k_0}{\beta} \right)^2 + \mathbf{k}^2 + M^2} \frac{1}{\left(\frac{2\pi p_0}{\beta} \right)^2 + \mathbf{p}^2 + M^2} \frac{e^{i \mathbf{k}_i \theta^{ij} \mathbf{p}_j}}{\left(\frac{2\pi k_0}{\beta} + \frac{2\pi p_0}{\beta} \right)^2 + (\mathbf{p} + \mathbf{k})^2 + M^2} \\
&= \frac{1}{\beta^2} \int_0^1 dw \int_0^\infty d\alpha_1 \alpha_1 \int_0^\infty d\alpha_2 \int d^3 \mathbf{l} d^3 \mathbf{p} e^{-\frac{1}{4\alpha_1} \tilde{\mathbf{p}}_i \tilde{\mathbf{p}}^i} e^{-(\alpha_2 + \alpha_1(w-w^2)) \mathbf{p}^2} e^{-\alpha_1 \mathbf{l}^2} e^{-(\alpha_1 + \alpha_2) M^2} \times \\
&\quad \sum_{k_0} \sum_{p_0} e^{-[\alpha_2 + \alpha_1(w-w^2)] \left(\frac{2\pi p_0}{\beta} \right)^2} e^{-\alpha_1 \left[\frac{2\pi k_0}{\beta} + (1-w) \frac{2\pi p_0}{\beta} \right]^2} \\
&= \frac{1}{\beta^2} \int_0^1 dw \int_0^\infty d\alpha_1 \alpha_1 \left(\frac{\pi}{\alpha_1} \right)^{\frac{3}{2}} \int_0^\infty d\alpha_2 e^{-(\alpha_1 + \alpha_2) M^2} \int d^3 \mathbf{p} e^{-\frac{1}{4\alpha_1} \tilde{\mathbf{p}}_i \tilde{\mathbf{p}}^i} e^{-(\alpha_2 + \alpha_1(w-w^2)) \mathbf{p}^2} \times \\
&\quad \sum_{k_0} \sum_{p_0} e^{-[\alpha_2 + \alpha_1(w-w^2)] \left(\frac{2\pi p_0}{\beta} \right)^2} e^{-\alpha_1 \left[\frac{2\pi k_0}{\beta} + (1-w) \frac{2\pi p_0}{\beta} \right]^2}, \tag{3.6}
\end{aligned}$$

in which $\tilde{\mathbf{p}}^i = \theta^{ij} \mathbf{p}_j$ and $\mathbf{l}_i = \mathbf{k}_i - (1-w) \mathbf{p}_i - \frac{i}{2\alpha_1} \tilde{\mathbf{p}}_i$.

We shall now integrate the momentum \mathbf{p} in Eqs.(3.5) and (3.6). To do this we first see that, because θ_{ij} is an antisymmetric matrix the U_{ij} matrix in the expression $\tilde{\mathbf{p}}_i \tilde{\mathbf{p}}^i = \mathbf{p}^i \theta_{ij} \theta^{jk} \mathbf{p}_k = \mathbf{p}^i U_i^k \mathbf{p}_k$ is symmetric. Then because any real, symmetric matrix can be diagonalized by an orthogonal matrix we can thus change the orthonormal variables \mathbf{p}_i into another orthonormal variables \mathbf{h}_i and find that

$$\begin{aligned}
& \frac{1}{4\alpha_1} \tilde{\mathbf{p}}_i \tilde{\mathbf{p}}^i + \alpha_2 \mathbf{p}^2 = \alpha_2 \mathbf{h}_1^2 + \left(\alpha_2 + \frac{\theta_{12}^2 + \theta_{23}^2 + \theta_{31}^2}{4\alpha_1} \right) (\mathbf{h}_2^2 + \mathbf{h}_3^2), \tag{3.7} \\
& \frac{1}{4\alpha_1} \tilde{\mathbf{p}}_i \tilde{\mathbf{p}}^i + (\alpha_2 + \alpha_1(w-w^2)) \mathbf{p}^2 = (\alpha_2 + \alpha_1(w-w^2)) \mathbf{h}_1^2 +
\end{aligned}$$

$$\left((\alpha_2 + \alpha_1(w - w^2)) + \frac{\theta_{12}^2 + \theta_{23}^2 + \theta_{31}^2}{4\alpha_1} \right) (\mathbf{h}_2^2 + \mathbf{h}_3^2). \quad (3.8)$$

Note that the orthonormal variables \mathbf{h}_i in Eq.(3.7) are different from those in Eq.(3.8).

Using the relations (3.7) and (3.8), Eqs.(3.5) and (3.6) become

$$\frac{1}{\beta^2} \int_0^\infty d\alpha_1 \int_0^\infty d\alpha_2 \frac{\pi}{\sqrt{\alpha_1 \alpha_2}} \frac{4\pi^2}{4\alpha_1 \alpha_2 + (\theta_{12}^2 + \theta_{23}^2 + \theta_{31}^2)} e^{-(\alpha_1 + \alpha_2)M^2} \sum_{p_0} e^{-\alpha_1 (\frac{2\pi p_0}{\beta})^2} \sum_{l_0} e^{-\alpha_1 (\frac{2\pi l_0}{\beta})^2}, \quad (3.9)$$

$$\frac{1}{\beta^2} \int_0^1 dw \int_0^\infty d\alpha_1 \int_0^\infty d\alpha_2 \frac{\pi \sqrt{\alpha_1}}{\sqrt{\alpha_2 + \alpha_1(w - w^2)}} \frac{4\pi^2 e^{-(\alpha_1 + \alpha_2)M^2}}{(\theta_{12}^2 + \theta_{23}^2 + \theta_{31}^2) + 4\alpha_1(\alpha_2 + \alpha_1(w - w^2))} \times \\ \sum_{k_0} \sum_{p_0} e^{-[\alpha_2 + \alpha_1(w - w^2)](\frac{2\pi p_0}{\beta})^2} e^{-\alpha_1 [\frac{2\pi k_0}{\beta} + (1-w)\frac{2\pi p_0}{\beta}]^2}. \quad (3.10)$$

respectively, after the integration of \mathbf{h}_i .

To proceed, let us first investigate Eq.(3.9).

$$(3.9) = \frac{1}{\beta^2} \int_0^\infty d\alpha_1 \int_0^\infty d\alpha_2 \frac{\pi}{\sqrt{\alpha_1 \alpha_2}} \frac{4\pi^2}{\theta_{12}^2 + \theta_{23}^2 + \theta_{31}^2} \left[1 + \sum_{n=1} \left(\frac{-4\alpha_2 \alpha_2}{\theta_{12}^2 + \theta_{23}^2 + \theta_{31}^2} \right)^n \right] \times \\ e^{-(\alpha_1 + \alpha_2)M^2} \sum_{p_0} e^{-\alpha_1 (\frac{2\pi p_0}{\beta})^2} \sum_{l_0} e^{-\alpha_1 (\frac{2\pi l_0}{\beta})^2} \\ = \frac{4\pi^4}{\theta_{12}^2 + \theta_{23}^2 + \theta_{31}^2} \frac{1}{M^2 \beta^2} \left[1 + O \left(\frac{\beta^2}{(\theta_{12}^2 + \theta_{23}^2 + \theta_{31}^2)M^2} \right) \right], \quad (3.11)$$

Therefore, when the thermal wavelength is smaller than the noncommutativity scale, i.e.

$$\frac{\beta^2}{(\theta_{12}^2 + \theta_{23}^2 + \theta_{31}^2)M^2} < 1,$$

then the first term in Eq.(3.11) is a good approximation. In a similar way we have the following approximation

$$(3.10) \approx \frac{1}{\beta^2} \int_0^1 dw \int_0^\infty d\alpha_1 \int_0^\infty d\alpha_2 \frac{\pi \sqrt{\alpha_1}}{\sqrt{\alpha_2}} \frac{4\pi^2}{(\theta_{12}^2 + \theta_{23}^2 + \theta_{31}^2)} e^{-(\alpha_1 + \alpha_2)M^2} \times \\ \sum_{k_0} \sum_{p_0} e^{-[\alpha_2 + \alpha_1(w - w^2)](\frac{2\pi p_0}{\beta})^2} e^{-\alpha_1 [\frac{2\pi k_0}{\beta} + (1-w)\frac{2\pi p_0}{\beta}]^2} \\ = \frac{2\pi^4}{\theta_{12}^2 + \theta_{23}^2 + \theta_{31}^2} \frac{1}{M^4 \beta^2}. \quad (3.12)$$

Substituting the above results into Eqs.(3.3) and (3.4) we finally find the nonplanar-diagram contributions of the effective potential

$$V(\phi_0)_{two\ loop}^{nonplanar} \approx \frac{\lambda \hbar^2}{1152\pi^2} \frac{1}{\theta_{12}^2 + \theta_{23}^2 + \theta_{31}^2} \frac{1}{\beta^2} \left(\frac{1}{M^2} - \frac{\lambda \phi_0^2}{2M^4} \right) \quad (3.13).$$

3.2 Planar Diagrams

The planar-diagram contributions of Eqs.(3.1) and (3.2) can be analyzed following Eqs.(3.9) and (3.10) after letting $\theta_{ij} = 0$. Thus, Eq.(3.1) with $\theta_{ij} = 0$ becomes

$$\begin{aligned} & \frac{\lambda}{\beta^2} \int_0^\infty d\alpha_1 \int_0^\infty d\alpha_2 \frac{\pi^3}{(\alpha_1 \alpha_2)^{\frac{3}{2}}} e^{-(\alpha_1 + \alpha_2)M^2} \sum_{p_0} e^{-\alpha_1 (\frac{2\pi p_0}{\beta})^2} \sum_{l_0} e^{-\alpha_2 (\frac{2\pi l_0}{\beta})^2} \\ &= \frac{\lambda}{\beta^2} \pi^3 \left[\int_0^\infty d\alpha \alpha^\epsilon \alpha^{-\frac{3}{2}} e^{-\alpha M^2} \sum_{p_0} e^{-\alpha (\frac{2\pi p_0}{\beta})^2} \right]^2 \\ &= \frac{\lambda}{\beta^2} \pi^3 \left[\Gamma(-\frac{1}{2} + \epsilon) \sum_{p_0} [(\frac{2\pi p_0}{\beta})^2 + M^2]^{\frac{1}{2} - \epsilon} \right]^2 \\ &= \frac{\lambda}{\beta^2} \pi^3 \left[\Gamma(-\frac{1}{2}) \right]^2 \left[\zeta(-1) \frac{4\pi M}{\beta} + M^2 (1 + O(\beta^2 M^2)) \right], \end{aligned} \quad (3.14)$$

which is consistent with that evaluated by Dolan and Jackiw [20]. Note that in above (and in the following, if it is necessary) we have added α^ϵ to regularize the integration over α . The infinite term appearing in the above equation has also been neglected, as it will give a temperature-independent contribution to the effective potential and could be absorbed by the counterterms for the renormalization requirement [20].

Note that, as it is difficult to evaluate Eq.(3.2) the authors in [20] considered the N -component scalar field theory, i.e. $\phi \rightarrow \phi_a$ with $a = 1, 2, \dots, N$. In this system the contributions of diagram (3.1) is $O(N^2)$ and diagram (3.2) $O(N)$. Thus in the large N approximation the diagram (3.2) can be neglected and the two-loop correction calculated in [20] is consistent with our result in Eq.(3.14). However, in obtaining the above result, as we have used the zeta regularization method [23] to perform the summation over the integral values of p_0 the calculations become easy and, in a similar way, we could also evaluate Eq.(3.2) in the high-temperature approximation.

Using the same method, Eq.(3.2) with $\theta_{ij} = 0$ becomes

$$\begin{aligned} & \frac{\lambda^2 \phi_0^2}{\beta^2} \int_0^1 dw \int_0^\infty d\alpha_1 \int_0^\infty d\alpha_2 \frac{\pi \sqrt{\alpha_1}}{\sqrt{\alpha_2 + \alpha_1(w - w^2)}} \frac{\pi^2}{\alpha_1(\alpha_2 + \alpha_1(w - w^2))} e^{-(\alpha_1 + \alpha_2)M^2} \times \\ & \frac{\lambda^2 \phi_0^2}{\beta^2} \sum_{k_0} \sum_{p_0} e^{-[\alpha_2 + \alpha_1(w - w^2)](\frac{2\pi p_0}{\beta})^2} e^{-\alpha_1[\frac{2\pi k_0}{\beta} + (1-w)\frac{2\pi p_0}{\beta}]^2} \end{aligned}$$

$$\begin{aligned}
&\approx \frac{\lambda^2 \phi_0^2}{\beta^2} \int_0^1 dw \int_0^\infty d\alpha_1 \int_0^\infty d\alpha_2 \frac{\pi \sqrt{\alpha_1}}{\sqrt{\alpha_2}} \frac{\pi^2}{\alpha_1 \alpha_2} e^{-(\alpha_1 + \alpha_2)M^2} \sum_{k_0} \sum_{p_0} e^{-\alpha_2 (\frac{2\pi p_0}{\beta})^2} e^{-\alpha_1 [\frac{2\pi k_0}{\beta} + (1-w)\frac{2\pi p_0}{\beta}]^2} \\
&= \frac{\lambda^2 \phi_0^2}{\beta^2} \pi^3 \Gamma(-\frac{1}{2}) \Gamma(\frac{1}{2}) \int_0^1 dw \sum_{k_0} \sum_{p_0} \left[(\frac{2\pi p_0}{\beta})^2 + M^2 \right]^{-\frac{1}{2}} \left[[\frac{2\pi k_0}{\beta} + (1-w)\frac{2\pi p_0}{\beta}]^2 + M^2 \right]^{\frac{1}{2}} \\
&= \frac{\lambda^2 \phi_0^2}{\beta^2} \frac{\pi^3}{4} \Gamma(-\frac{1}{2}) \Gamma(\frac{1}{2}) [1 + O(\beta^2 M^2)].
\end{aligned} \tag{3.15}$$

Substituting the above results into Eqs.(3.1) and (3.2) we finally find the planar-diagram contributions of the effective potential

$$V(\phi_0, N)_{two\ loop}^{planar} = -\lambda \hbar^2 \frac{M}{293\pi\beta^3} (1 + O(\beta^2 M^2)). \tag{3.16}$$

3.3 Effective Potential and Symmetry Property

Combining Eqs.(3.13) and (3.16), we find that the high-temperature effective potential is

$$V(\phi_0)_{two\ loop} \approx -\lambda \hbar^2 \frac{M}{293\pi\beta^3} + \frac{\lambda \hbar^2}{1152\pi^2} \frac{1}{(\theta_{12}^2 + \theta_{23}^2 + \theta_{31}^2) \beta^2} \left(\frac{1}{M^2} - \frac{\lambda \phi_0^2}{2M^4} \right). \tag{3.17}$$

From the above result we see that at high temperature in which the thermal wavelength is smaller than the noncommutativity scale the planar-diagram contributions will dominate. This is the conclusion of this paper. The remaining part of this paper is to investigate the property of the nonplanar contribution. From Eq.(3.13) we see that

$$\frac{\partial V(\phi_0)_{two\ loop}^{nonplanar}}{\partial(\phi_0^2)} \approx \frac{\lambda \hbar^2}{1152\pi^2} \frac{-\lambda m^2}{(\theta_{12}^2 + \theta_{23}^2 + \theta_{31}^2) \beta^2 M^6}. \tag{3.18}$$

The above equation tells us that, if $m^2 > 0$, i.e., the symmetry is not broken in the tree level, then the value $\partial V(\phi_0)_{two\ loop}^{nonplanar} / \partial(\phi_0^2)$ becomes negative for all values of ϕ_0^2 . This means that the nonplanar diagram has an inclination to induce radiatively symmetry breaking if it is not broken in the tree level.

On the other hand, if $m^2 < 0$, i.e., the symmetry has been spontaneously broken in the tree level, then because the value of $M^6 = (m^2 + \frac{1}{2}\lambda\phi_0^2)^3$ can become negative for small value of ϕ_0^2 we therefore see that the value $\partial V(\phi_0)_{two\ loop}^{nonplanar} / \partial(\phi_0^2)$ in Eq.(3.18) is negative too. This means that the nonplanar diagram does not have an inclination to restore the symmetry breaking at high temperature, in contrast to the conventional believing that high temperature could restore the symmetry breaking. Note that the investigation in [20] had found that the O(N)-invariant scalar model which is radiatively broken will remain broken at high temperature, while which is broken at tree level can be restored at high temperature.

In the next subsection we will evaluate the planar diagrams in zero space. We will see that the nonplanar-diagram corrections in the three space behave like those in the planar diagrams in zero space, at high temperature. Thus we can explain this property as a consequence of the drastic reduction of the degrees of freedom in the nonplanar diagrams at high temperature.

3.4 Planar Diagram at Zero space and Dimensional Reduction of Nonplanar Diagram

The calculations of diagrams (3.1) and (3.2) at zero space dimension are

$$\begin{aligned}
 [Diagram (3.1)]_{zero\ space\ dimension} &= \frac{2}{3} \frac{\hbar^2 \lambda}{24 \beta^2} \left(\sum_{k_0} \frac{1}{\left(\frac{2\pi k_0}{\beta}\right)^2 + M^2} \right)^2 \\
 &= \frac{2}{3} \frac{\hbar^2 \lambda}{24 \beta^2 M^4} \left(1 + O(\beta^2 M^2) \right). \tag{3.19}
 \end{aligned}$$

$$\begin{aligned}
 [Diagram (3.2)]_{zero\ space\ dimension} &= -\frac{1}{2} \frac{\hbar^2 \lambda^2 \phi_0^2}{36 \beta^2} \sum_{k_0} \sum_{p_0} \frac{1}{\left(\frac{2\pi k_0}{\beta}\right)^2 + M^2} \times \\
 &\quad \frac{1}{\left(\frac{2\pi p_0}{\beta}\right)^2 + M^2} \frac{1}{\left(\frac{2\pi k_0}{\beta} + \frac{2\pi p_0}{\beta}\right)^2 + M^2} \\
 &= -\frac{1}{2} \frac{\hbar^2 \lambda^2 \phi_0^2}{36 \beta^2 M^6} \left(1 + O(\beta^2 M^2) \right), \tag{3.20}
 \end{aligned}$$

in which the zeta regularization method has been used to perform the summations over integral values p_0 and k_0 . (Note that there is no nonplanar diagram in the zero-space theory.)

The important difference between the theory at three spaces dimension and that at zero space is that, in the former system the contribution of the planar-diagram part of Eq.(3.1), calculated in Eq.(3.14), is proportional to β^{-3} while that in the later system, calculated in Eq.(3.19), is proportional to β^{-2} . The calculation in Eq.(3.11), however, find that the high-temperature two-loop correction from the nonplanar diagrams in three-space theory is proportional to β^{-2} , which therefore behaves as the Feynman diagram in zero-space theory.

In the same way of comparison, the high-temperature two-loop correction from the nonplanar diagram of Eq.(3.4) in three-space theory, calculated in Eq.(3.12), is proportional to β^{-2} , which does behave like as the Feynman diagram in zero-space theory, calculated in Eq.(3.20).

Therefore, we can conclude that there is the drastic reduction of the degrees of freedom in the nonplanar diagram at high temperature. This is because that, at high temperature for which the thermal wavelength is small than the noncommutativity scale, there is no way to distinguish and count the contributions of modes to the nonplanar-diagram contribution in the effective potential. To confirm the above argument we would like to analyze the $\lambda\phi^3$ theory in the next section.

4 Two-Loop Corrections: $\lambda\phi^3$ Theory

It is known that in $\lambda\phi^3$ theory there is only one diagram in the two-loop level, as that given in Eq.(3.2). Thus we need only to analyze this equation in this section. For the $\lambda\phi^3$ theory in three space dimensions it is easy to see that, up to an irrelevant constant, the

contributions from the planar diagram and the nonplanar diagram are like that in the $\lambda\phi^4$ theory in three space dimensions. Thus the property of the reduction of degrees of freedom at high temperature is also shown in this system.

Let us now turn to the $\lambda\phi^3$ theory in five space dimensions. The space noncommutative, for simplicity, is chosen as

$$\begin{pmatrix} 0 & 0 & 0 & 0 & 0 & 0 \\ 0 & 0 & \theta_{12} & \theta_{13} & 0 & 0 \\ 0 & \theta_{21} & 0 & \theta_{23} & 0 & 0 \\ 0 & \theta_{31} & \theta_{32} & 0 & 0 & 0 \\ 0 & 0 & 0 & 0 & 0 & \theta \\ 0 & 0 & 0 & 0 & -\theta & 0 \end{pmatrix}, \quad (4.1)$$

which means that the extra noncommutative two spaces, with noncommutativity θ , are commutate to the other noncommutative three spaces.

Following the prescriptions in section 3 we can find from Eq.(3.6) the corresponding contribution of the nonplanar diagram:

$$\begin{aligned} & \frac{\lambda^2 \phi_0^2}{\beta^2} \sum_{k_0} \sum_{p_0} \int d^5 \mathbf{k} d^5 \mathbf{p} \frac{1}{\left(\frac{2\pi k_0}{\beta}\right)^2 + \mathbf{k}^2 + M^2} \frac{1}{\left(\frac{2\pi p_0}{\beta}\right)^2 + \mathbf{p}^2 + M^2} \frac{e^{i\mathbf{k}_i \theta^{ij} \mathbf{p}_j}}{\left(\frac{2\pi k_0}{\beta} + \frac{2\pi p_0}{\beta}\right)^2 + (\mathbf{p} + \mathbf{k})^2 + M^2} \\ & \approx \frac{\lambda^2 \phi_0^2}{\beta^2} \int_0^1 dw \int_0^\infty d\alpha_1 \int_0^\infty d\alpha_2 \frac{\pi}{\sqrt{\alpha_1}} \frac{\pi}{\sqrt{\alpha_2}} \frac{4\pi^2}{(\theta_{12}^2 + \theta_{23}^2 + \theta_{31}^2)} \frac{\pi^2}{\theta^2} e^{-(\alpha_1 + \alpha_2)M^2} \times \\ & \quad \sum_{k_0} \sum_{p_0} e^{-[\alpha_2 + \alpha_1(w-w^2)]\left(\frac{2\pi p_0}{\beta}\right)^2} e^{-\alpha_1\left[\frac{2\pi k_0}{\beta} + (1-w)\frac{2\pi p_0}{\beta}\right]^2} \\ & = \frac{\lambda^2 \phi_0^2}{\beta^2} \frac{4\pi^6}{\theta_{12}^2 + \theta_{23}^2 + \theta_{31}^2} \frac{1}{\theta^2 M^2} \left[1 + O\left(\frac{\beta^2}{(\theta_{12}^2 + \theta_{23}^2 + \theta_{31}^2)M^2}\right) \right]. \end{aligned} \quad (4.2)$$

In a similar way, we can find from Eq.(3.15) the corresponding contribution of the planar diagram:

$$\begin{aligned} & \frac{\lambda^2 \phi_0^2}{\beta^2} \sum_{k_0} \sum_{p_0} \int d^5 \mathbf{k} d^5 \mathbf{p} \frac{1}{\left(\frac{2\pi k_0}{\beta}\right)^2 + \mathbf{k}^2 + M^2} \frac{1}{\left(\frac{2\pi p_0}{\beta}\right)^2 + \mathbf{p}^2 + M^2} \frac{1}{\left(\frac{2\pi k_0}{\beta} + \frac{2\pi p_0}{\beta}\right)^2 + (\mathbf{p} + \mathbf{k})^2 + M^2} \\ & \approx \frac{\lambda^2 \phi_0^2}{\beta^2} \int_0^1 dw \int_0^\infty d\alpha_1 \int_0^\infty d\alpha_2 \frac{\pi^5 e^{-(\alpha_1 + \alpha_2)M^2}}{(\alpha_1 \alpha_2)^{\frac{3}{2}}} \sum_{k_0} \sum_{p_0} e^{-[\alpha_2 + \alpha_1(w-w^2)]\left(\frac{2\pi p_0}{\beta}\right)^2} e^{-\alpha_1\left[\frac{2\pi k_0}{\beta} + (1-w)\frac{2\pi p_0}{\beta}\right]^2} \\ & = \frac{\lambda^2 \phi_0^2 \pi^6}{\beta^2} \left[-\frac{2\pi M}{\beta} + M^2 \left(1 + O(\beta^2 M^2) \right) \right]. \end{aligned} \quad (4.3)$$

We thus see that the high temperature behavior of the nonplanar diagram for the $\lambda\phi^3$ theory living on five space dimensions, i.e. Eq.(4.2), has a similar temperature dependence to that living on zero space dimension, i.e. Eq.(3.20). Note that all the properties found in section 3 could also be shown in the $\lambda\phi^3$ at five space dimensions.

5 Conclusion

In this paper we have evaluated the high-temperature renormalized effective potential for the scalar field theory in the noncommutative spacetime to the two-loop approximation. We have considered the $\lambda\phi^4$ theory in the three space dimensions and $\lambda\phi^3$ theory in the five space dimensions. As the space-time noncommutativity ($\theta_{0i} \neq 0$) will lead to a non-unitary theory [18], we have considered only space noncommutative theories.

Using the path-integration formulation we see that there is no nonplanar diagram in the one-loop potential. Thus the spontaneous symmetry breaking is blind to the noncommutativity at this level. The nonplanar parts can appear in the two-loop level but they do not have an inclination to restore the symmetry breaking in the tree level. This property is in contrast to the conventional believing that high temperature could restore the symmetry breaking. To explain this phenomena we compare the result with the effective potential in the zero-space dimension and explain this property as a consequence of the drastic reduction of the degrees of freedom in the nonplanar diagram at high temperature in which the thermal wavelength is smaller than the noncommutativity scale [15]. Our results show that the nonplanar two-loop contribution to the effective potential can be neglected in comparison with that from the planar diagrams.

In this paper we only consider the noncommutative scalar field theory. For the more realistic model, such as that including the Yang-Mills field, there are more diagrams to be evaluated to find the effective potential. However, we believe that the property of the reduction of the degrees of freedom in the nonplanar diagram at high temperature will also be shown in other models. It remains to be investigated.

1. A. Connes, M. R. Douglas and A. Schwarz, *Noncommutative Geometry and Matrix Theory: Compactification on Tori*, JHEP **02** (1998) 003, hep-th/9711162;
M.R. Douglas, C. Hull, *D-branes and the Noncommutative Torus*, JHEP **02** (1998) 008, hep-th/9711165.
2. M. M. Sheikh-Jabbari, *More on Mixed Boundary Conditions and D-branes Bound States*, Phys. Lett.**B 425** (1998) 48, hep-th/9712199;
F. Ardalan, H. Arfaei, M.M. Sheikh-Jabbari, *Mixed Branes and M(atrix) Theory on Noncommutative Torus*, hep-th/9803067; *Noncommutative Geometry From Strings and Branes*, JHEP **02** (1999) 016, hep-th/9810072; *Dirac Quantization of Open Strings and Noncommutativity in Branes*, Nucl. Phys. **B576** (2000) 578, hep-th/9906161.
3. N. Seiberg and E. Witten, *String Theory and Noncommutative Geometry*, JHEP **09**, 032 (1999), hep-th/9908142.
4. C-S. Chu, P-M. Ho, *Noncommutative Open String and D-brane*, Nucl. Phys. **B550** (1999) 151, hep-th/9812219; *Constrained Quantization of Open String in background B Field and Noncommutative D-brane*, Nucl. Phys. **B568** (2000) 447, hep-th/9906192;
T. Lee, *Canonical Quantization of Open String and Noncommutative Geometry*, Phys. Rev **D 62** (2000) 024022, hep-th/9911140.
5. T. Filk, *Divergences in a Field Theory on Quantum Space*, Phys. Lett. **B376** (1996) 53;
B. A. Campbell and K. Kaminsky, *Noncommutative Field Theory and Spontaneous symmetry breaking*, Nucl. Phys. **B 581** (2000) 240, hep-th/0003137.
6. S. Minwalla, M. Van Raamsdonk, N. Seiberg, *Noncommutative Perturbative Dynamics*, JHEP **02** (2000) 020, hep-th/9912072.
7. I. Ya. Aref'eva, D.M. Belov, A.S. Koshelev, *Two-Loop Diagrams in ϕ^4 Theory*, Phys. Lett. **B476** (2000) 431, hep-th/9912075;
A. Micu and M. M. Sheikh-Jabbari, *Noncommutative ϕ^4 Theory at Two loop*, hep-th/0008057.
8. W. H. Huang, *Two-Loop Effective Potential in Noncommutative scalar field theory*, Phys. Lett.**B 496** (2000) 206, hep-th/0009067.
9. C.P. Martin, D. Sanchez-Ruiz, *The One-loop UV Divergent Structure of U(1) Yang-Mills Theory on Noncommutative R^4* , Phys. Rev. Lett. **83** (1999) 476, hep-th/9903077.
10. M.M. Sheikh-Jabbari, *One Loop Renormalizability of Supersymmetric Yang-Mills Theories on Noncommutative Two-Torus*, JHEP **06** (1999) 015, hep-th/9903107;
T. Krajewski, R. Wulkenhaar, *Perturbative quantum gauge fields on the noncommutative torus*, Int. J. Mod. Phys. **A15** (2000) 1011, hep-th/9903187;
A. Matusis, L. Susskind, N. Toumbas, *The IR/UV Connection in the Noncommutative Gauge Theories*, JHEP **12** (2000) 002, hep-th/0002075;
M. Hayakawa, *Perturbative analysis on infrared aspects of noncommutative QED on*

- R^4 , Phys. Lett. **B478** (2000) 394, hep-th/9912094; *Perturbative analysis on infrared and ultraviolet aspects of noncommutative QED on R^4* , hep-th/9912167.
11. H. S. Snyder, Phys. Rev. **71** (1947) 38; **72** (1947) 68.
 12. Connes, *Noncommutative Geometry* Academic. Press, New York, 1994); Connes A. *Gravity coupled with matter and the foundation of non commutative geometry*, Comm. in Math. Phys. **182** (1996) 155, hep-th/9603053;
Landi G. *An introduction to noncommutative spaces and their geometries*, Lecture Notes in Physics, Springer-Verlag , hep-th/97801078;
Schücker T. *Geometries and forces*, Summer School *Noncommutative geometry and applications*, Lisbon September 1997, hep-th/9712095 .
 13. S. Nam, *Casimir Force in Compact Noncommutative Extra Dimensions and Radius Stabilization*, JHEP **10** (2000) 044, hep-th/0008083;
J. Gomis, T. Mehen and M.B. Wise, *Quantum Field Theories with Compact Noncommutative Extra Dimensions*, JHEP **08** (2000) 029; hep-th/0006160;
W. H. Huang, *Casimir Effect on the Radius Stabilization of the Noncommutative Torus*, Phys. Lett.**B 497** (2001) 317; hep-th/0010160;
W. H. Huang, *Finite-Temperature Casimir Effect on Radius Stabilization of the Noncommutative Torus*, JHEP **11** (2000) 041, hep-th/0011037.
 14. G. Arcioni and M. A. Vazquez-Mozo, *Thermal effects in perturbative noncommutative gauge theories*, JHEP **01** (2000) 028;
G. Arcioni, J.L.F. Barbon, Joaquim Gomis and M. A. Vazquez-Mozo, *On the stringy nature of winding modes in the noncommutative thermal field theories*, JHEP **06** (2000) 038, hep-th/0004080.
 15. W. Fischler, E. Gorbatov, A. Kashani-Poor, S. Paban, P. Pouliot and J. Gomis, *Evidence for Winding States in Noncommutative Quantum Field Theory*, JHEP **05** (2000) 024, hep-th/0002067;
W. Fischler, E. Gorbatov, A. Kashani-Poor, R. McNees, S. Paban, P. Pouliot and J. Gomis, *The interplay between θ and T* , JHEP **06** (2000) 032, hep-th/0003216.
 16. R.-G. Cai and N. Ohta, *On the thermodynamics of large N Noncommutative Super Yang-Mills Theory*, Phys. Rev. **D 61** (2000) 124012, hep-th/9910092.
 17. J. Gomis, K. Landateiner, and E. Lopez, *Nonrelativistic Non-commutative Field Theories and UV/IR Mixing*, Phys. Rev. **D 62** (2000) 105006, hep-th/0004115.
 18. J. Gomis and T. Mehen, *Spacetime Noncommutative Field Theories and Unitarity*, Nucl. Phys. **B 591** (2000) 265, hep-th/0005129;
N. Seiberg, L. Susskind, N. Toumbas, *Space/Time Non-Commutativity and Causality*, JHEP **06** (2000) 044, hep-th/0005015.
 19. R. Jackiw, Phys. Rev. **D 9** (1974) 1686.

20. L. Dolan and R. Jackiw, Phys. Rev. **D 9** (1974)3320.
21. H. Weyl. Z. Physik, **46** (1927) 1.
22. J. E. Moyal, Proc. Cambridge Philo. Soc. **45** (1949) 99.
23. E. Elizalde, S. D. Odintsov, A. Romeo, A. A. Bytsenko, and Zerbini, *Zeta Regularization Techniques with Applications*, World Scientific, (1994).